Coupling excavator hydraulic system and internal combustion engine models for the real-time simulation

Coupling excavator hydraulic system and internal combustion engine models for the Real-Time simulation

Paolo Casoli[1,*], Agostino Gambarotta[1], Nicola Pompini[1] and Luca Riccò[1]

[1] *Industrial Engineering Department, University of Parma Italy, Parco Area delle Scienze 181/A, 43124 Parma (PR) ITALY*

[*] Corresponding Author: e-Mail: paolo.casoli@unipr.it
Tel.: +39-0521-905868; Fax: +39-0521-905705.

Abstract: Rising energy costs and emissions restrictions force manufacturers to exploit new techniques to reduce fuel consumption and pollutant production. Many solutions have been proposed for off-road vehicles, mainly based on reduction of hydraulic losses, better control strategies and introduction of hybrid architectures. In these applications the optimization of the matching between hydraulic system and thermal engine is a major concern to improve system overall efficiency. The work presented in the paper is focused on the development of a method for the simulation of typical mobile machinery where hydraulic systems are powered by internal combustion engines; the proposed co-simulation approach can be useful in the development cycle of this machinery.

Keywords: "Control-oriented" Modelling; Hydraulic Excavator; Variable Displacement Pump; Co-simulation of complex systems; Modelling.

1. Introduction

Fuel consumption and pollutant emissions are and will continue to be the driving forces in the improvement of vehicles, i.e., cars, trucks as well as earth movers and construction machines. These aspects are amplified by more stringent emissions regulations that nowadays are going to impact also off-highway vehicles development. Many solutions have been proposed recently to reduce the energy consumption of off-road vehicles, mainly based on reduction of hydraulic losses, better control strategies of hydraulic systems and the introduction of hybrid architectures [1, 2, 3]. For off-road vehicles, the energy storage systems of an hybrid architectures could be electric batteries or hydraulic accumulators. If electric batteries have high energy density, hydraulic accumulators show higher power density and energy conversion efficiency that are needed to effectively recover mechanical energy [4, 5, 6]. A number of proposals can be found in the literature for the development of Hydraulic Hybrid Systems (HHS), as reported in [6, 7, 8].

In the mentioned applications, the optimization of the matching between hydraulic system and internal combustion engine is one of the major concerns for the improvement of system overall efficiency and the reduction of fuel consumption. Virtual design based on mathematical models is a widely used option to match system components making the best use of their operating characteristics. Generally speaking, this is the case when dealing with complex systems, where the ability to simulate interactions between system components in real operating conditions is a primary concern for the optimization of system layout and management. When dealing with the simulation of hydraulic circuits and primary engines several problems arise, and this is probably the reason why up to now in most of the proposed models of hydraulic off-road vehicles thermal engine is not considered or otherwise is modelled following map-based approaches (several examples can be found in [3, 6, 7, 8, 9, 10, 11, 12]), with very few and recent exceptions [13].

Mathematical models have been used within several steps of the design process in systems engineering, but with the continuing increase of computers power and the improvement of computational methods, simulation tools are currently used in every phase of the development cycle (the so-called V-cycle [14]). Usually, models with different levels of detail – and therefore with different complexity – are used at each stage of the development process. In the concept stage, very fast, low fidelity models are required for rapid architecture and concept analysis, while coming to an exhaustive design and optimization of components and sub-systems, detailed 1-D to 3-D models are used. Faster, lower fidelity models are employed for the system integration phase, and for the development and testing of control systems (i.e., ECU, control strategies, etc.) through XiL (MiL, SiL and HiL) tools.

As a matter of fact, modelling tasks carried out throughout the development cycle involve very often the use of disparate simulation tools, each committed to a specific sub-system (e.g., AMESim® for the hydraulic system, GT-Power®, Boost® or Simulink® for the engine, in the case of an HHS or a hydraulic excavator). Even if a single simulation tool may be considered within all stages of the development process, actually this approach seems to require significant efforts in terms of costs and time.

The work presented in this paper is focused on the development of methods and techniques for mathematical simulation of typical mobile machinery where hydraulic systems are powered by internal combustion engines (ICEs).

By coupling models of a Diesel engine and the hydraulic circuit of an excavator by carefully handling causality, I/O parameters and co-simulation issues, a comprehensive mathematical model was set up and used to simulate steady and transient behaviour of the system. Different integration time steps were defined for the two sub-models taking account of their differing numerical “stiffness”, thus allowing to run the comprehensive model faster than real time.

A potential of this approach is the ability to develop a comprehensive control strategy for the whole system, with the possibility to maximize performance and reduce fuel consumption in relation to the specific tasks for the system itself was developed; rather than considering the overall system as the sum of components, whose control strategies are optimized in reference to the execution of generic tasks, the general control strategy can be developed to maximize the performance of the individual components in the specific configuration adopted. The proposed models allow for the simulation of the whole system taking account of non-linear and dynamic behaviour of its components still running in Real-Time. Thanks to this, these models can be used within the design process both to define the

system layout and to design and test related control strategies (since they can be embedded in XiL systems).

The engine model has been built in Simulink® following a "crank-angle" 0D, lumped-parameter approach and allows to take account of non-linearities and low-order dynamics typical of Diesel engines[25, 35]. The model of the hydraulic system was set up in AMESim® coupling the models of all involved components (axial piston pump, flow compensators, valves, actuators, etc.) to replicate the non-linear behaviour of the system with the typical fast dynamic. Kinematics of the system (e.g., arms, boom, bucket, etc.) were simulated using the proper AMESim® libraries [15, 18]. The developed models were coupled to co-simulate the behaviour of an excavator and the comprehensive model was validated comparing several calculated output with the first experimental data gathered on a real machine.

Results reported in the paper show to what extent the proposed co-simulation approach, based on dynamic model for both the hydraulic system and the internal combustion engine, could be useful in the control strategy development phase for hydraulic systems powered by Diesel engines.

2. Modelling of Hydraulic System

The hydraulic system considered is based on a typical circuit of an excavator composed of a variable displacement axial piston pump with flow and pressure compensators, flow control valves and hydraulic actuators as described in [18]. Kinematics of the system (e.g., arms, boom, bucket, etc.) will be taken into account in the next future.

2.1 Variable displacement axial piston pump model

The pump considered in the paper is a variable displacement axial piston pump, fig. 1. The comprehensive pump model includes three sub-models: the pressure compensator (PC), the flow compensator (FC) and the flow generator model.

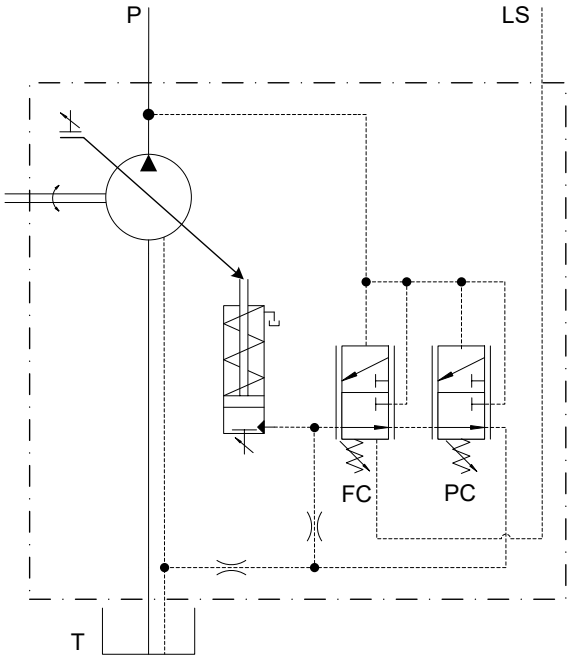

Fig.1. *Pump ISO scheme*

2.1.1 Pressure and flow compensators models.

The main purpose of the pressure compensator (PC) is to limit maximum value of system pressure (P line) when it is greater than a defined relief setting pressure. When this situation occurs the PC causes a rotation of the swash plate, reducing the flow rate and avoiding further increases of the system pressure. The task of the flow compensator (FC) is to offset pump displacement for a defined preload value by controlling the swash plate angle. As a common practice, a "load-sensing" pump is designed to keep a constant pressure drop across a controlling orifice in order to regulate fluid mass flow rate. In order to avoid wasting energy, the FC adjusts the pump displacement until the pump outlet pressure is greater than the load pressure of a defined quantity. The model used in this research was already presented in [15], in this work has been used a slightly simplified version of the original model where small redundant chambers and leakages, having limited effects on the pump dynamic behaviour, according to the Activity Index criteria [39, 40]. The corresponding volume increase of the remaining chambers had a positive effect to reduce numerical stiffness of the resulting model, according with Eq.(4) which clearly shows that hydraulic components have a considerably small time constant, due to the fact that even low flow rates induce high variations in chambers pressure (since mineral oils have high bulk modulus, β~17000 bar).

2.1.2 Flow generator model

Several examples of pump modelling have been reported in literature [21,22, 23], but they are more suitable for internal pump's components optimization rather than for modelling the behaviour of a pump working in complex systems. In this paper, the approach followed for the modelling is that of considering the pump as a simple flow generator for which the volumetric flow rate is calculated from the rotational speed and the pump instantaneous displacement, geometrically related to the swash plate angular position:

$$\dot{V}_{th} = V_d(\alpha)\, n \tag{1}$$

where $\dot{V}_{th}$ is the theoretical volumetric flow rate, α is the swash plate angular position, V_d the pump displacement, and n is the shaft rotational speed.

A black box model, based on experimental data, was adopted for the evaluation of the barrel torque, being the flow characteristic of the pump correlated to the equilibrium of the swash plate.

This was achieved by measuring the pressure in the pump actuator (which controls the corresponding actuator torque) for given values of pump outlet pressure and swash plate angular positions, and keeping the rotational speed fixed. A correlation between the pressure in the pump actuator and pump outlet pressure was consequently identified. The authors experimentally found a linear correlation between the control piston pressure and the system pressure, as already reported in [15].

Hydro-mechanical and volumetric efficiencies have been evaluated experimentally [24] and a correlation between η_{hm}, η_v and rotational speed, delivery pressure and swash plate displacement was identified. The real flow outlet is thereby calculated as:

$$\dot{V} = \eta_v(p_{sys}, n, \alpha) \cdot \dot{V}_{th} \tag{2}$$

and the torque required at the shaft is:

$$T = \frac{\Delta p \cdot V_d(\alpha)}{2\pi} \cdot \frac{1}{\eta_{hm}(p_{sys}, n, \alpha)} \tag{3}$$

Where p_{sys} is the pump outlet pressure; Δp is the pressure increment through the pump.

The pump model was developed in AMESim® environment. Fig. 2 reports the sketch of the model.

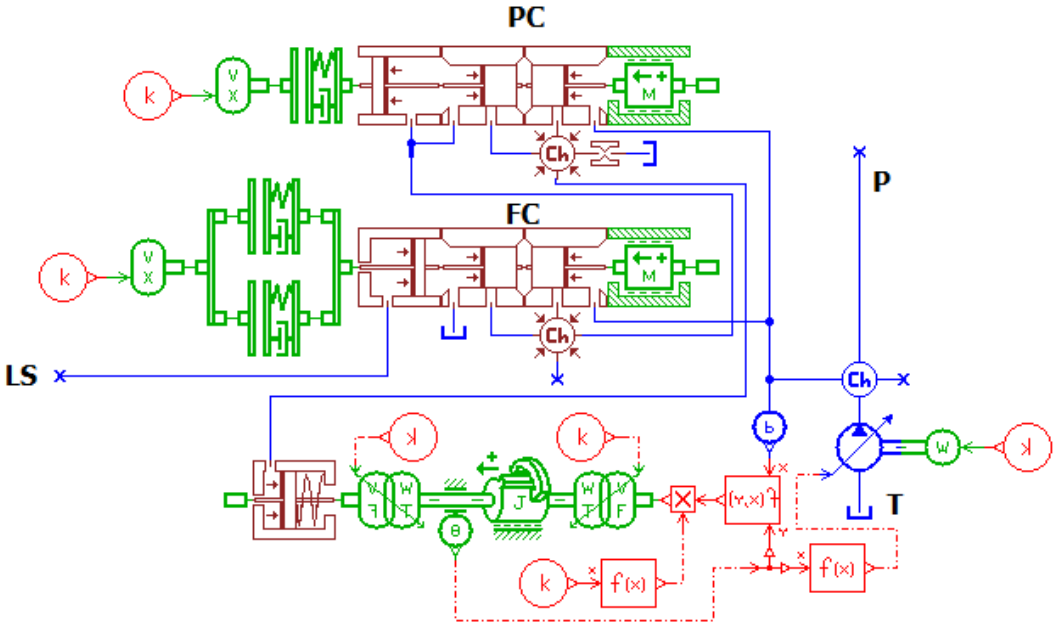

Fig.2. *AMESim® sketch of the pump model*

2.2 Directional Valve Model

The considered excavator is equipped with a load sensing flow sharing valve block (Walvoil® DPX series). The valve section ISO scheme is reported in fig.3. The main tasks of the valve block are to govern the outlet flow rate through each single control section to the corresponding actuator, to extrapolate the LS pressure and to keep a constant pressure drop across the main spool metering area providing the flow sharing operation condition when required.

Usually, during a digging cycle, when the front excavation tool are operated, at least three valve sections are used at the same time, and the pump may work in flow saturation conditions (i.e., the pumps flow rate is lower than the flow required by the system to keep the required pressure across the metering areas); if this situation occurs, the load sensing flow sharing valve block still allows the operator to control safely the system, but with the excavation tool components velocities reduced. The valve's pressure compensator maintains a constant pressure drop across the spool metering area, so the result is a flow to the working port that still depends only on the spool position.

Each single valve section was modelled as a white box model and validated by comparison with experimental results as reported in [18].

The valve mathematical model is based on the interaction between a fluid-dynamic model (FDM) and a mechanical-geometrical model (MGM). The FDM allows the evaluation of pressures inside each control volume and the corresponding flow rates between adjacent volumes, while the MGM calculates the dynamic equilibrium of the spools estimating its positions and the corresponding orifices flow areas. Both the FDM and the MGM are based on a lumped parameter approach. In order to apply

the FDM and the MGM to the valve, the control volumes considered are reported in figs. 4, 5. Pressure distribution inside each control volume is assumed uniform and varying with time with a derivative that can be obtained combining continuity equation and state equation of the fluid:

$$\frac{dp_i}{dt} = \frac{\beta}{\rho_i}\frac{1}{V_i(x)}\left(\sum \dot{m} - \rho_i \frac{dV_i(x)}{dt}\right) \tag{4}$$

where for the i^{th} control volume p is the absolute pressure, β is the bulk modulus, $\dot{m}$ is the mass flow rate, ρ is the fluid density and $V(x)$ is the volume, x is the instantaneous position of the spool. Constant fluid temperature is assumed. Fluid density is evaluated as a function of pressure as described in [19, 20]. The summation in eq.(4) represents the net mass flow rate entering or leaving a volume, obtained considering the contribution of all orifices connected with the considered volume. Mass flow rate through the orifices is calculated using the generalized Bernoulli's equation in quasi-steady flow conditions:

$$\dot{m} = \rho\, C_d\, A(x) \sqrt{\frac{2\,|\Delta p|}{\rho}} \tag{5}$$

where C_d is the discharge coefficient and $A(x)$ is the flow area. A proper saturated value for the discharge coefficient of each connection was defined on the basis of experimental data or using values reported in literature [19]. Thereafter the instantaneous value of the discharge coefficient is evaluated as a function of Reynolds number to account for partially developed or fully turbulent conditions. Annular leakages past spool bodies were neglected.

The MGM calculates the instantaneous position and velocity of the spool from Newton's second law estimating forces acting on the spool (i.e., hydrostatic forces, spring force, friction forces, hydrodynamic forces). Static and dynamic friction forces are evaluated by use of the Karnopp friction model and considering the Stribeck effect, static and dynamic friction coefficients are assumed constant, while hydrodynamic forces are neglected.

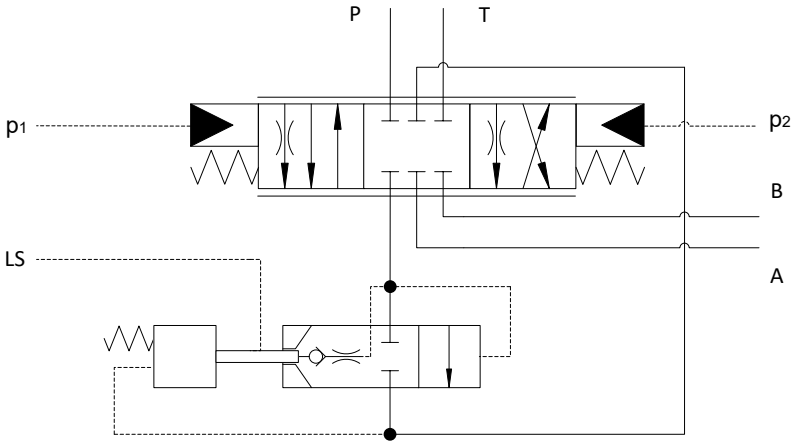

Fig.3. *ISO scheme of the valve section.*

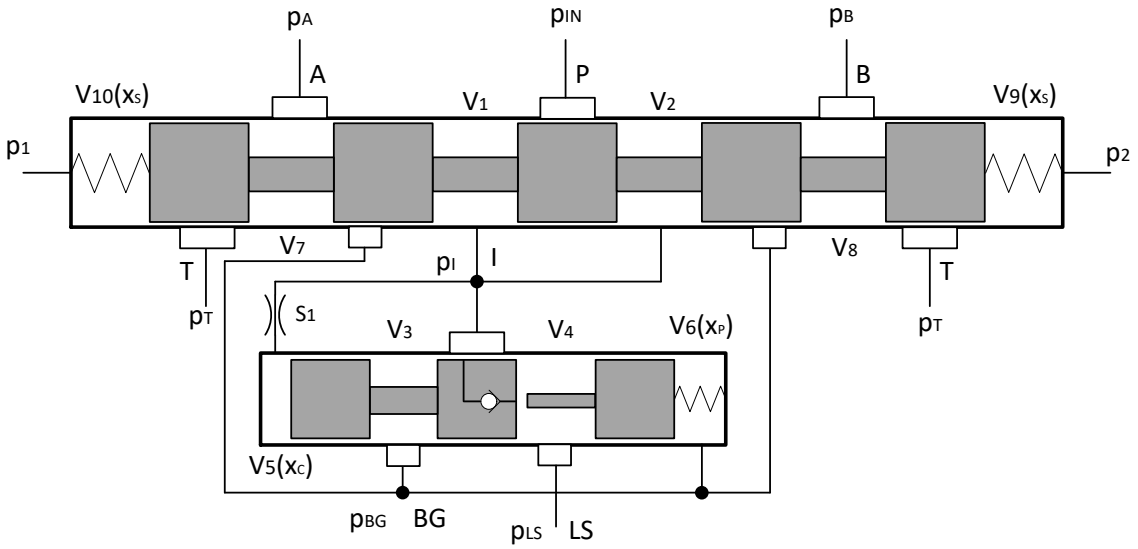

Fig.4. *Schematic drawing of the valve section.*

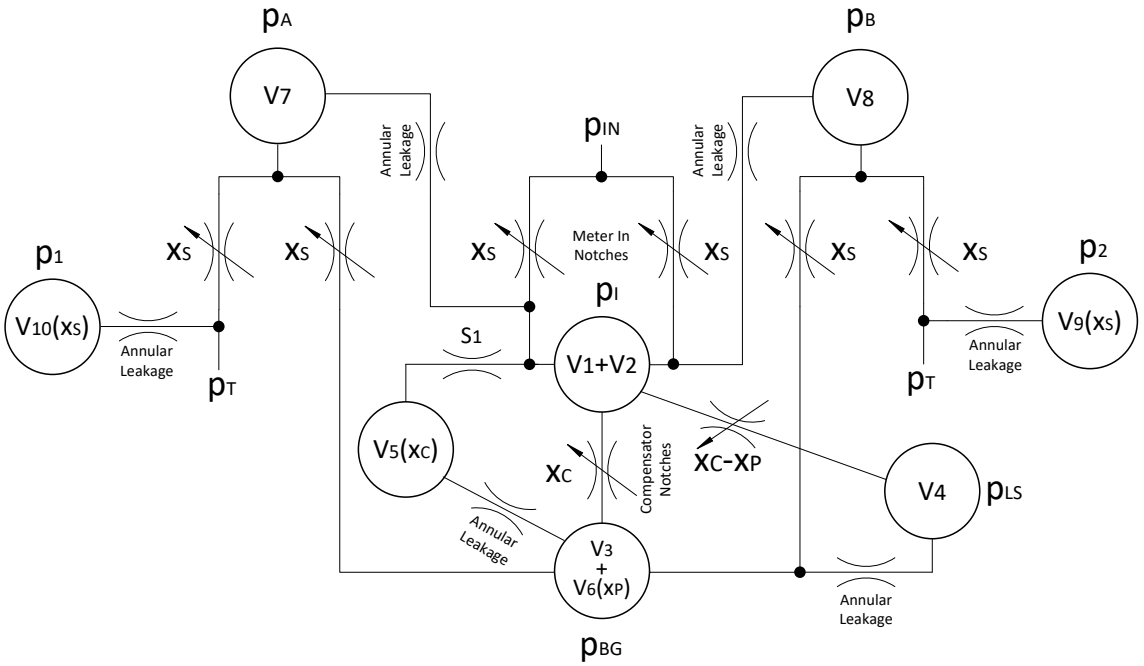

Fig.5. *Scheme of the valve section - fluid dynamic model.*

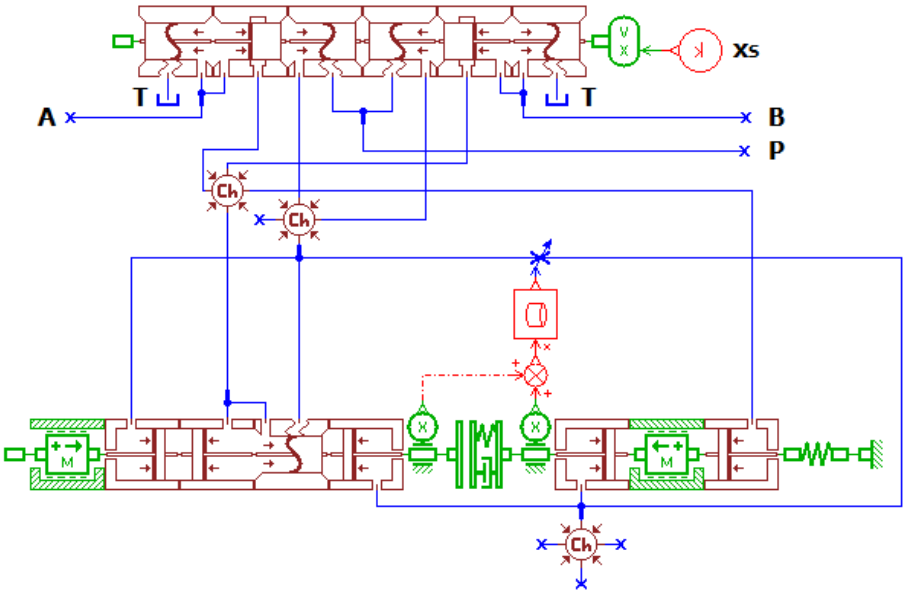

Fig.6. *AMESim® sketch of the valve model*

The valve's model was realized using the AMESim® Hydraulic and Mechanical library, fig.6.

3. Modelling of the Diesel engine: methods and used approach.

Several mathematical models are proposed in the open literature for the fast simulation Internal Combustion Engines [25, 26]. In the development of any comprehensive engine model, simplifications and approximations have to be properly introduced in order to simulate the real behaviour of the whole system as a consequence of the behaviour of its components. When "Real-Time" models are required, physical –and chemical– principles (generally based on conservation laws) have to be combined with empirical descriptions of processes and components taking account of relevant aspects and avoiding a detailed description of the others [25, 26].

Mean Value Models (MVMs) for the simulation of engines transients can be developed through a proper alternation of Filling and Emptying (F&E) and Quasi-Steady Flow (QSF) methods [27, 28], that allows taking account of low frequency processes which dominate engine behaviour. The use of F&E and QSF methods in the development of 0D, lumped parameters MVMs can be structured following specific criteria in order to avoid numerical problems in the simulation [29]. System components can be classified as *volume components* or *capacitances*, modelled through the use of state-space representations and *non-volume components* or *resistances*, modelled through algebraic equations. The dynamic behaviour of the system results from the interactions between capacitances and resistances.

The simulation of in-cylinder processes introduces well-known difficulties, especially for Diesel engines, where combustion is highly non-homogeneous. When dealing with the simulation of "cycle-to-cycle" phenomena (typically intake and exhaust flows and combustion process) F&E and QSF methods can still be used, but more complex models usually result, whose equations have to be integrated on a crank angle base. Calculation time is usually a challenge in this case, since the estimation of in-cylinder pressure and temperature histories requires more detailed approaches than those used for black-box models [25, 30]. The complexity of chemical and physical processes occurring in the cylinder cannot be described in detail: for fast applications simplified 0D single-zone

models [26, 27, 28] seem still the best option. In-cylinder processes can be simulated on a crank-angle base following a F&E approach joined with a QSF technique for gas flows through valves by applying the energy and mass conservation equations to a gas mixture which is considered homogeneous within the cylinder ("single-zone" models). Similar models have been proposed for control-oriented applications [27, 32] and used in several "crank-angle" commercial tools.

Within this scenario, a "crank-angle" model of a four-cylinder turbocharged Diesel engine based on a single-zone scheme has been developed by the authors, and integrated within the previously developed original library [17, 32, 33].

3.1. The simulation library for the development of I.C. Engines Mean Value Models.

The simulation library built up by the authors in the last decade has been conceived to create "Real-Time" Mean Value Models (MVMs) of automotive engines. Based on F&E and QSF methods, and developed within MATLAB®/Simulink® environment to improve portability and flexibility, the library has been organised in a hierarchical structure so that sub-model blocks can be found, picked up and assembled following the desired system layout. Dedicated procedures have been defined for the identification of each block [34].

Intake and exhaust system components were modelled as volume components (i.e., capacitances) through a F&E approach (e.g., manifolds), or as non-volume components (i.e., resistances) with a QSF methodology (e.g., valves, compressors, turbines, etc.) [32, 33]. Processes which take place in the cylinder have been modelled through a F&E method based on mass and energy conservation equations applied following a single-zone approach to an open thermodynamic system in the well-known form of mass and energy conservation equations, where the working fluid is assumed to be a mixture of ideal gases.

Combustion contribution to energy conservation equation has been estimated from Watson's formulation of fuel burn fraction *FB* [27, 28]:

$$FB(\theta) = \beta \cdot f_p(\theta) + (1-\beta) \cdot f_d(\theta) \tag{6}$$

The fuel burn rate, function of the crank angle θ, is composed of two terms, f_p and f_d, representing the pre-mixed and diffusive phases of the combustion. The shape of these two curves, which depends on engine operating condition (e.g. engine shaft speed) is reported in literature [27, 28].

The coefficient β in eq. (11), the so-called "phase proportionality factor", is evaluated as:

$$\beta = 1 - \frac{a \cdot \phi^b}{{\tau_{id}}^c} \tag{7}$$

where ϕ is the overall fuel air ratio and τ the ignition delay, evaluated through Hardenberg and Hase correlation [29]). Coefficients *a*, *b*, and *c* are estimated from experimental data.

In-cylinder equations are integrated on a crank angle base instead than time, with an angle step of 1 deg to avoid numerical problems. As the corresponding time step to 1 deg angle step would be too little to perform fast simulations (~86 μs at 2000 r/min), the whole model uses an higher sample time, 1 ms, and in-cylinders equations are iteratively integrated n-times during a single time step in order to obtain the required crank angle resolution. During the iterative integration, boundary conditions for the in-cylinder process (e.g. engine speed, manifold pressure) are assumed to stay constant, while the

resulting output from the integration (e.g mass flow rates to the manifolds) are properly averaged in order to ensure mass and energy conservation [17].

Piston and crank inertial effect on shaft dynamics are neglected, accounting only for the slow dynamics on the mechanical part of the model.

Figure 7 depicts a causality diagram for the ICE, obtained by assembling the components contained in the library by the authors.

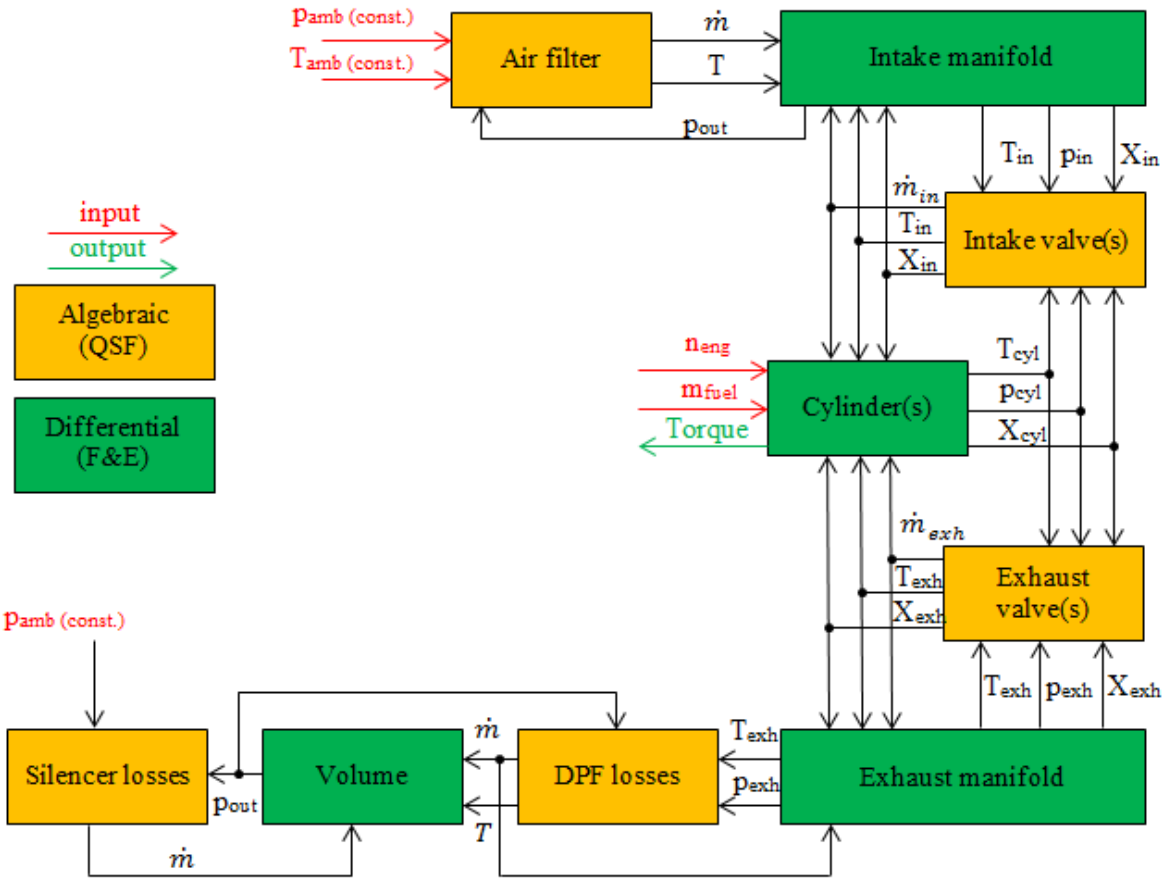

Fig.7. *Causality scheme for the four-cylinder naturally aspirated Diesel engine.*

3.2. Engine model calibration

The application considered in the present work equips a four cylinder direct injection, naturally aspirated, midsize Diesel engine, developed by Yanmar® (Tab.1,). The engine is equipped with an electric governor that controls the mass of injected fuel to reduce the error between measured and desired engine rotational speed. In Figs. 8 and 9 engine power output, brake torque, and BSFC characteristic curves given by Yanmar are reported.

Tab.1. *Engine characteristics parameters*

Type	four-strokes, inline, water cooled, Diesel
No. of cylinders – Bore x Stroke [mm]	4 – 98 x 110
Combustion system	direct injection
Compression ratio	18.5
Displacement [cm^3]	3319
Rated output [kW] @ 2200 r/min	46.3
Specific fuel consumption [g/kWh] @ 2200 r/min	240
Max Torque [Nm] @ 1400 r/min	228
Fuel injection timing [deg BTDC] @ 2200 r/min	13

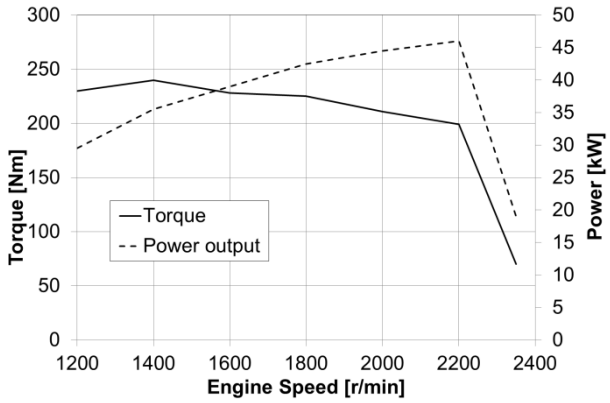

Fig.8. *Engine power and torque characteristics.*

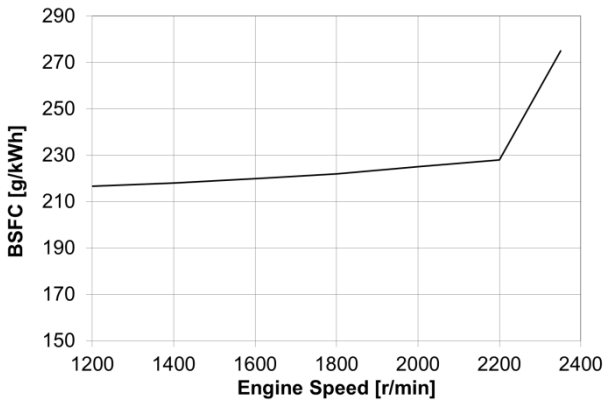

Fig.9. *BSFC characteristics.*

Input parameters of the overall engine model are ambient temperature and pressure (assumed as constants), rotational speed and injected fuel mass. The model allows the evaluation of every operating and state parameter (e.g., power output, temperature and composition of exhaust gases, bmep, etc.). As shown in fig.10, the engine controller adjusts the mass of injected fuel in order to track the target rotational speed in spite of changes in load torque.

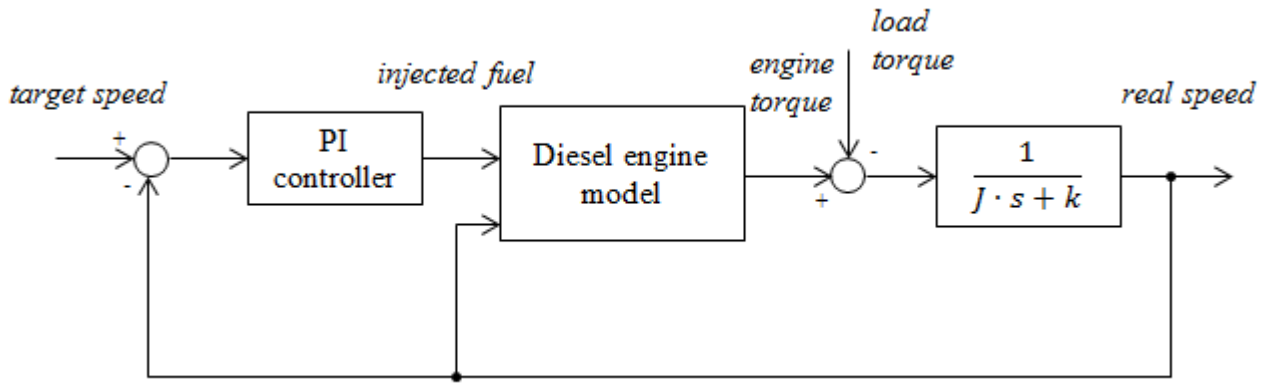

Fig.10. *Schematic of the engine-load control.*

The overall engine model was then identified on the basis of steady-state experimental data from Yanmar with the aim to obtain the expected values for BSFC and power output for given values of engine speed and fuel mass flow rate (figs.8 and 9). Parameters *a*, *b* and *c* in eq.(12) were tuned to obtain the maximum engine torque at 2200r/min corresponding to a start of injection (SOI) of 13degCA, as stated on the engine data sheet. In other operating conditions the SOI has been tuned to the minimum value corresponding to the maximum output torque. Following the usual tuning procedures to obtain the maximum efficiency [36], effects of SOI on torque output were estimated by the model (fig.11) then allowing defining the optimal SOI value (fig.12).

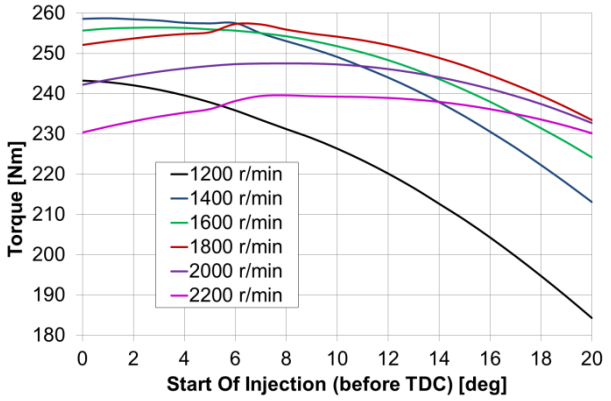

Fig.11. *Simulated torque output vs. SOI for different engine speeds.*

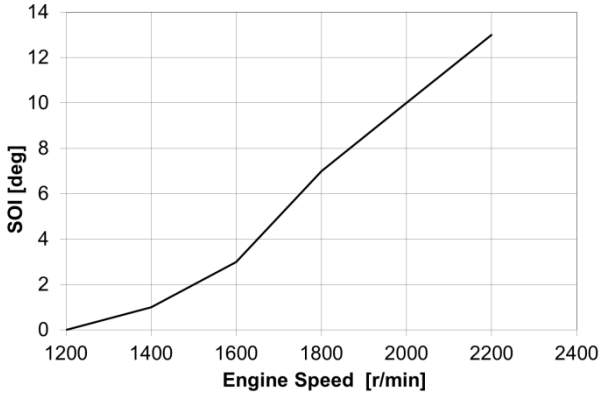

Fig.12. *Defined map of SOI [degCA] as a function of rotational speed.*

The engine model was finally validated by comparing simulated torque characteristic with experimental data given by the OEM. Results reported in fig.13 show a satisfactory agreement, with errors below 5% and the overall trend reproduced adequately.

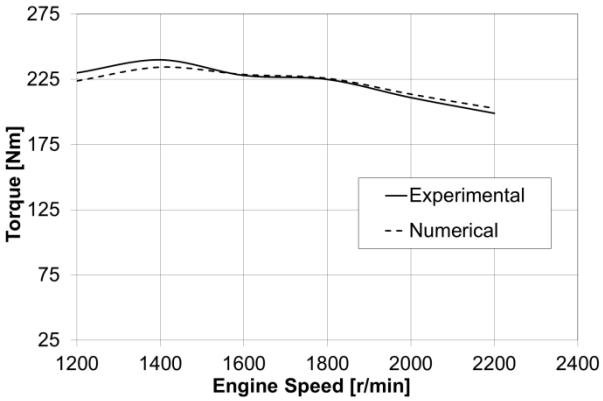

Fig.13. *Simulated and experimental engine torque characteristic.*

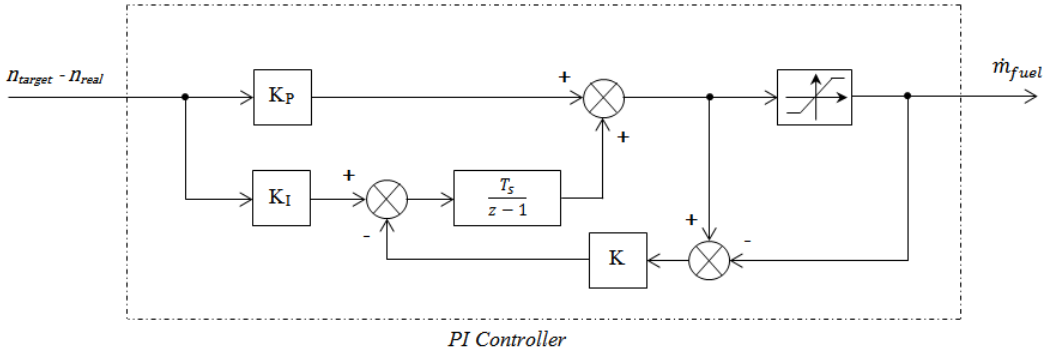

Fig.14. *PI Controller Scheme.*

The engine control strategy has been implemented as a very simple PI controller with saturation and tracing anti-windup back calculation [38], fig.14, where the proportional gain (K_P), the integral gain (K_I) and the back tracking gain (K) have been calibrate on the following limitations specified by the engine OEM:

- while the load changes from 100% to 0, a maximum engine speed overshoot of 12% of the rated value (2200r/min) is accepted, maximum steady state error over engine speed is imposed equal to 6.8% of the rated value;
- a maximum rise time of 6s is allowed by the OEM.

4. Coupling Hydraulic System and Engine models: the comprehensive excavator model.

The models of the hydraulic circuit and the internal combustion engine have been properly coupled together complying with causality to develop a typical excavator system mathematical model [25]. The kinematic has not been taken into account during this phase, and in order to replicate realistic loads and flow rates on the valve, the experimental data measured during the operating cycle (described in section 5) have been imposed to the valve's ports (i.e. p_{load} and X_{spool}). Fig.15 reports the scheme of the simulated model, where the internal combustion engine and the hydraulic mathematical models are physically linked taking account of balance of momentum at the engine shaft and of shaft dynamics. Load torque is evaluated from eq.(7), depending on pump mass flow rate (i.e. on swash plate angular position α) and delivery pressure, while the engine define an engine torque (Eng Torque) mean value over the cycle. The approach used for both models does not consider high frequency behaviors, therefore the overall model is able to take account of low frequency interactions between the hydraulic system and the engine.

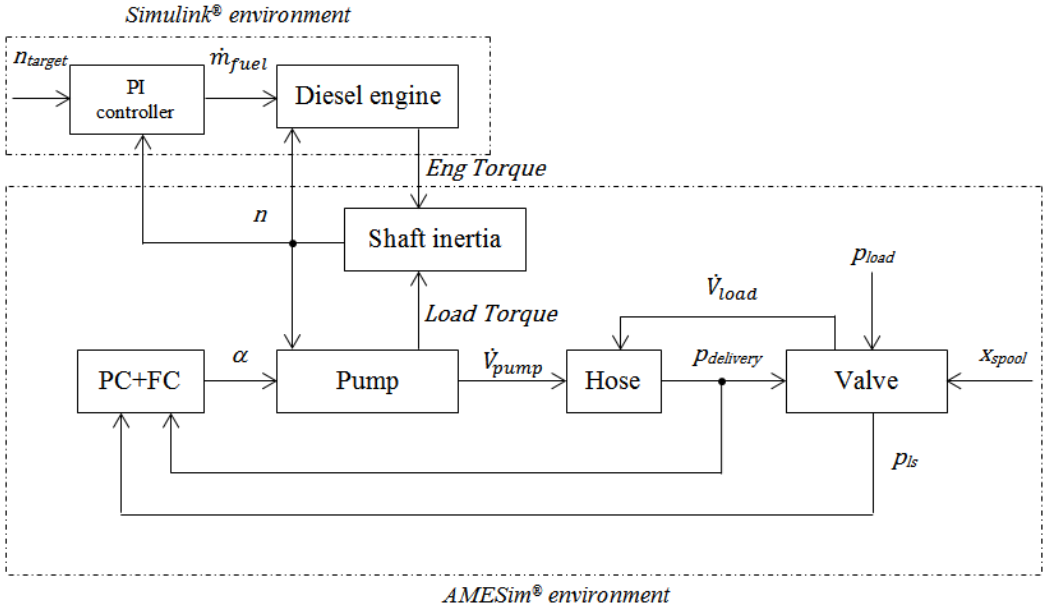

330

331 ***Fig.15.*** *Sketch of the simulation model with internal combustion engine and hydraulic system.*

332 In order to evaluate the advantages of having a dynamic model of the engine coupled with the
333 hydraulic system instead of a constant speed model, during the control algorithm definition procedure,
334 the simulation model reported in fig.16 have been defined.

335 The experimental data and the simulation results of the two models have been compared in section
336 5.

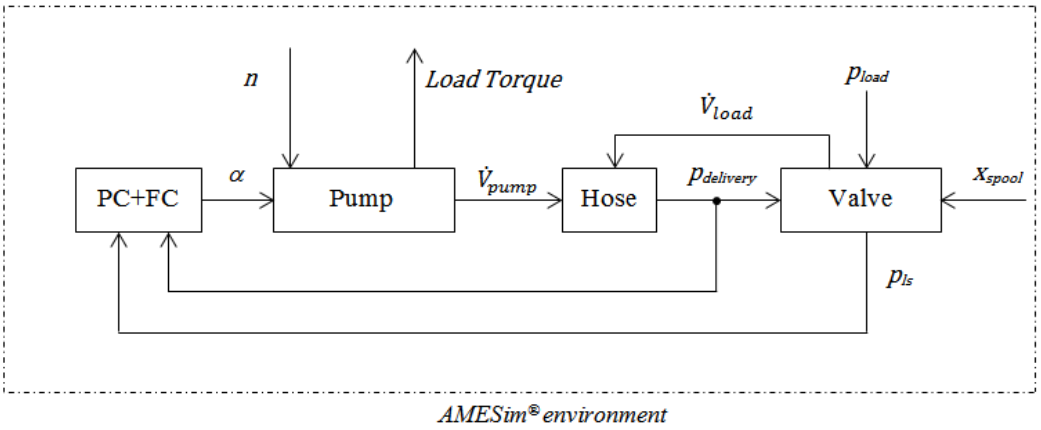

337

338 ***Fig.16.*** *Sketch of the simulation model with the hydraulic system only.*

339

340 Since engine and hydraulic system models were developed using two different simulation tools (i.e.,
341 Simulink® and AMESim®), the latter has been reduced to an "S-Function" and imported into
342 Simulink® environment [40]. Equations of both models were solved using Euler fixed step method
343 adopting two different time steps, i.e., 2ms for the engine model and about 80ns for the hydraulic
344 circuit to avoid numerical instabilities which usually arise when solving with a fixed step method a
345 stiff set of equations. This is due to the faster dynamics of the hydraulic system caused by the high
346 bulk modulus of the working fluid.

347 With these specifications, the complete model proved to run on a 2.2GHz Quad Core Pentium PC
348 with 8GB RAM reaching a satisfying ratio of computation time over physical time (always lower than
349 0.9).

5. Experimental activity and model validation.

In order to validate the proposed mathematical model, a preliminary dedicated experimental activity was carried out on a middle size (9 ton) excavator (fig.17) equipping the engine and the hydraulic circuit previously described. The bucket actuator was instrumented to measure the pressures inside the actuator's chambers during the operated working cycle, while the boom and the arm actuators were not instrumented. Other operating parameters of interest were measured (see tab.2) to assess system response and performance during the testing cycles. Data was acquired with a sample frequency of 100Hz to capture properly transient behaviour of the system.

Tab.2. *Operating parameters measured during the experimental investigation.*

Parameter	*Sensor*
Pump delivery pressure, $p_{delivery}$	Strain gauge
Load Sensing pressure, p_{LS}	Strain gauge
Bucket actuator pressure, p_{load}	Strain gauge
Swash angle, α	LVDT

Fig.17. *The middle size excavator considered in the experimental activity.*

The working cycle considered during this working phase involved just the bucket movement. Starting from the fully extended position, the operator acted on the valve control joystick moving the valve spool to completely extend the actuator piston, therefore closing the bucket. Afterward, the actuator piston was moved backward to return the bucket in the initial position and the cycle could be repeated.

In order to study the behaviour of the system, with particular reference to the engine, the described working cycle has been carried out for two values of the target engine speed n_{target}, i.e., 1480r/min (case 1) and 1750r/min (case 2).

Measured data were compared with theoretical results from the mathematical models described in section 4. Input parameters for the models (see section 4) are the valve spool opening position x_{spool}, the bucket actuator pressure p_{load} and the engine target velocity n_{target}.

In order to show the advantages of having a dynamic model of the internal combustion engine coupled with the dynamic model of the hydraulic system, the experimental measured data were compared with the simulation results obtained with both the model showed in fig.14 (with the engine model) and the model showed in fig. 15 (with the pump rotating at a constant speed, i.e. without the engine model). Figs.18 and 19 show the measured time histories of the spool position x_{spool} for case 1 and case 2 respectively. In figs.20 and 21 the experimental time histories of bucket actuator pressures p_{load} for both cases are reported.

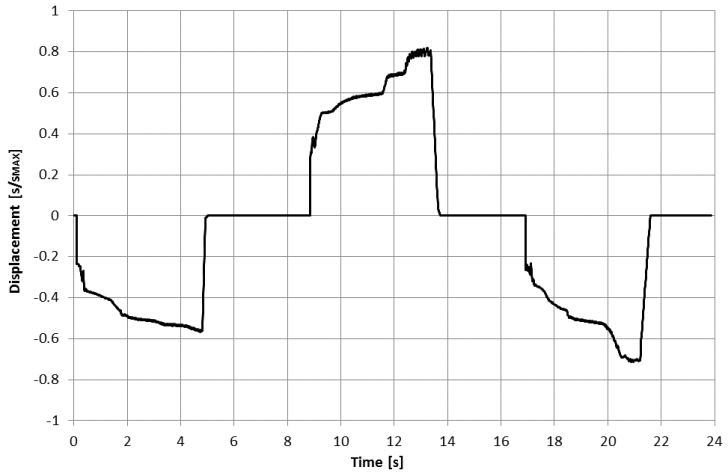

Fig.18. *Valve spool opening position x_{spool} measured during the working cycle and used as input for the simulation (case 1).*

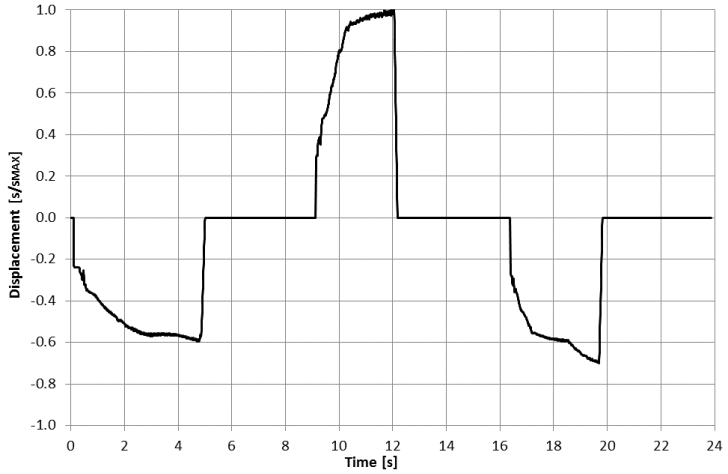

Fig.19. *Valve spool opening position x_{spool} measured during the working cycle and used as input for the simulation (case 2).*

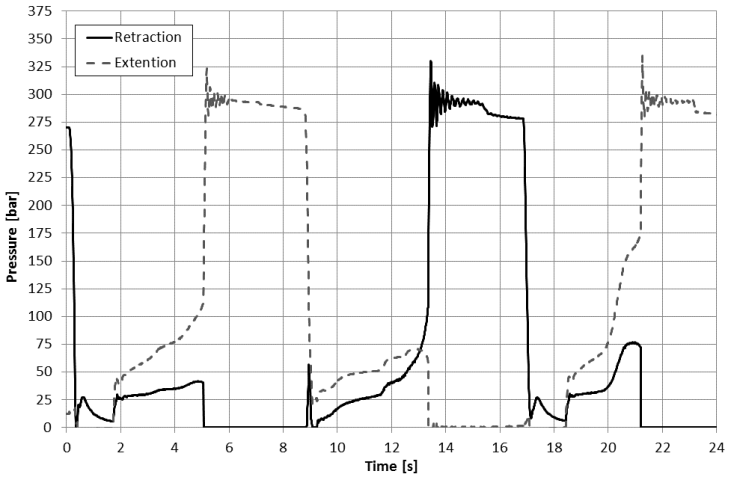

Fig.20. *Bucket actuator chambers pressures p_{load} measured during the working cycle and used as input for the simulation (case 1).*

383

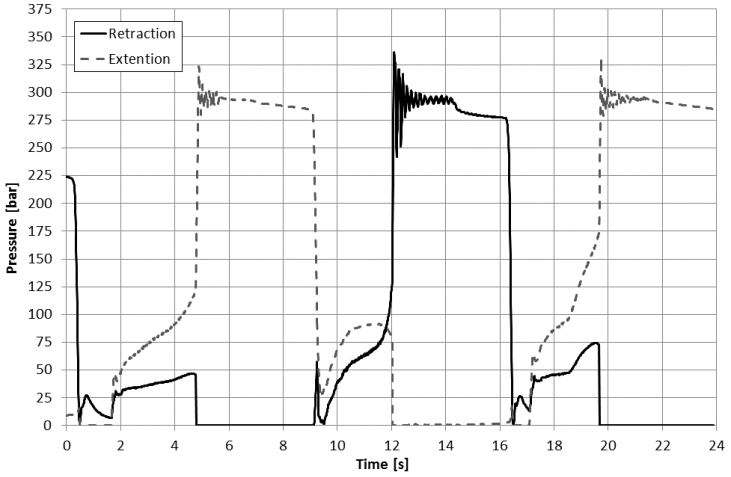

Fig.21. *Bucket actuator chambers pressures p_{load} measured during the working cycle and used as input for the simulation (case 2).*

384

385 Experimental data and simulation results are compared in figs.22÷24 for a target velocity n_{target}
386 equal to 1480 r/min (case 1) and in figs.26÷29 for a target velocity n_{target} equal to 1750 r/min (case 2).
387 Both the models were able to estimate p_{LS} changes during considered transients for both target
388 speed values, as shown in figs.22 and 26. Comparing fig.20 with fig.22 it is evident that the actual
389 pressure measured in the actuator chamber p_{load} is slightly different from the actual pressure p_{LS}: this
390 pressure loss is due to hydraulic line resistance (considered in the model of the hydraulic circuit). It
391 should be noted that the valve defines the pressure p_{LS} only when the main spool is open, and therefore
392 when the operator closes the valve orifice p_{LS} drops nearly to zero. The same considerations can be
393 recalled when comparing figs.21 and 26. Anyway, results reported in figs.22 and 26 show the
394 capabilities of the proposed mathematical model to reproduce the real regulator behaviour, being the
395 curves almost overlapped.
396 Small differences can be also pointed out with reference to pump delivery pressure $p_{delivery}$, as
397 shown in figs.23 and 27, for the studied cases.
398 Observing figs. 24 and 28, where the comparison between experimental and simulation results for
399 the swash plate angle position α are reported, it is possible to notice the advantages on having a

dynamic model of the internal combustion engine coupled with the hydraulic system, instead of simply setting a constant velocity source for the pump. In fact when the operator opens or closes quickly the valve's main spool, a variation on the shaft speed occurs, as reported in figs. 25 and 29. In these situations the pump's regulator defines a new swash plate position in order to meet the hydraulic system pressure demand while the engine PI controller acts in order to keep the shaft speed at the reference value.

The mathematical model with the engine shows simulated engine speed transients trends very similar to experimental data, figs. 25 and 29, and better results are showed for the swash plate angle position too, compared with the mathematical model without the engine dynamic model.

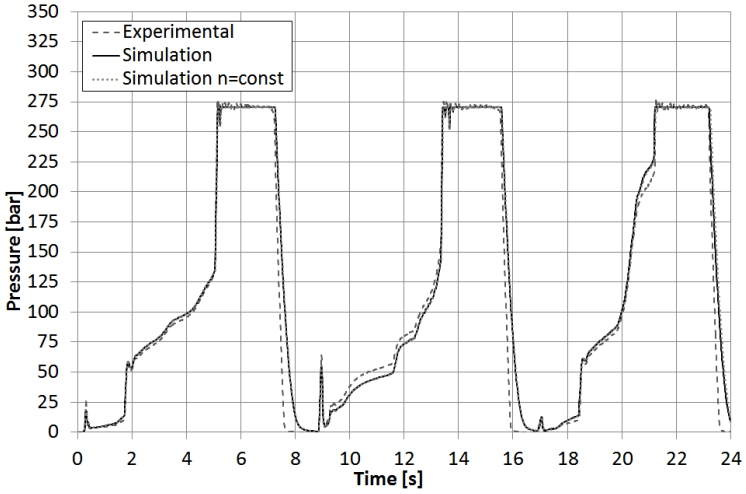

Fig.22. *Measured and calculated transients for p_{LS} (case 1).*

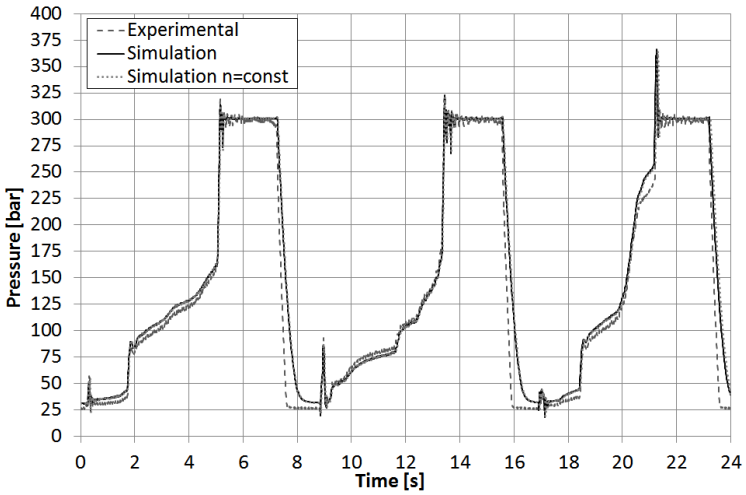

Fig.23. *Measured and calculated transients for $p_{delivery}$ (case 1).*

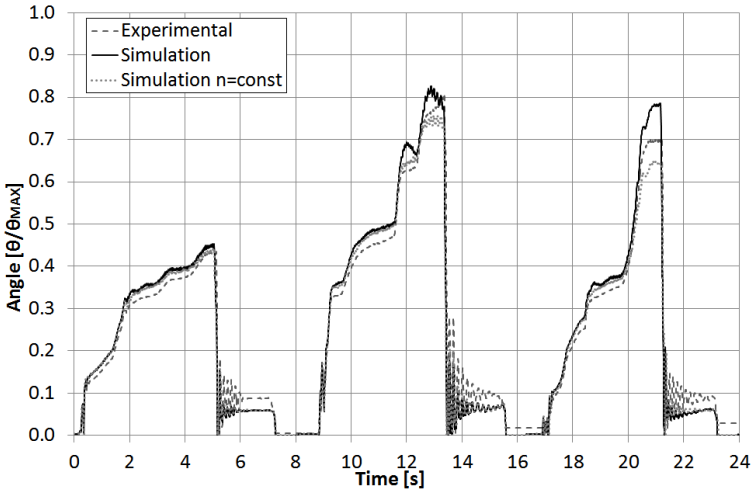

Fig.24. *Measured and calculated transients for swash plate angle α (case 1).*

412

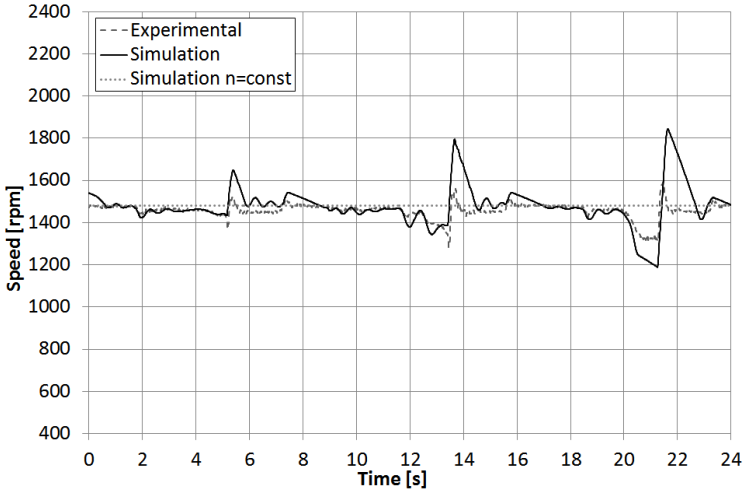

Fig.25. *Measured and calculated transients for engine speed (case 1).*

413

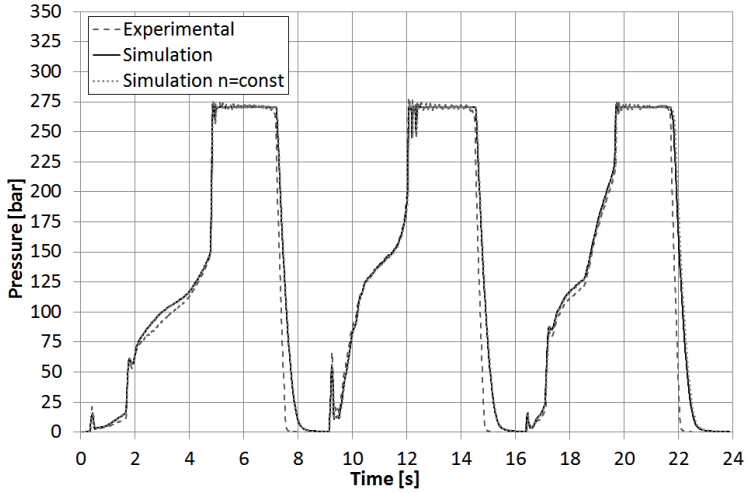

Fig.26. *Measured and calculated transients for p_{LS} (case 2).*

414

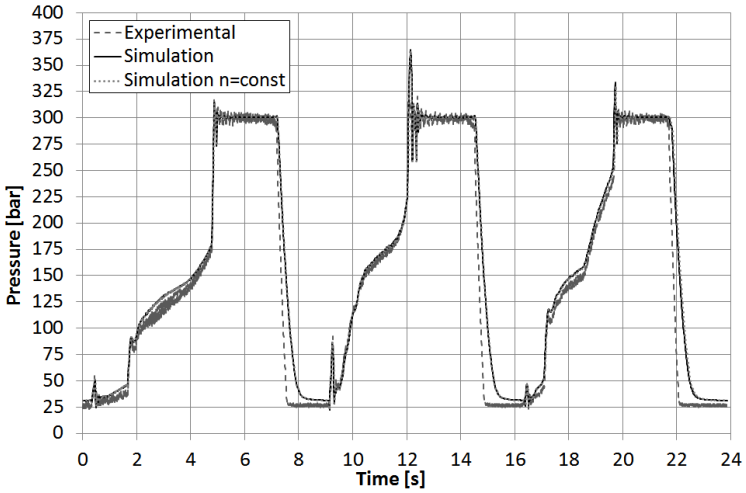

Fig.27. *Measured and calculated transients for* $p_{delivery}$ *(case 2).*

415

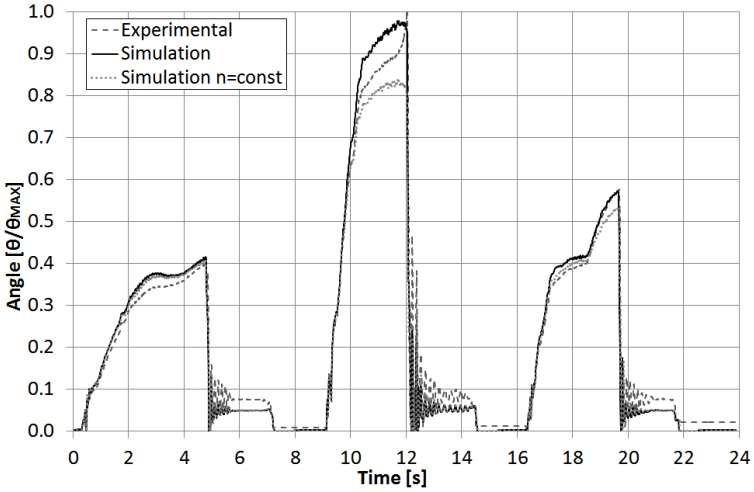

Fig.28. *Measured and calculated transients for swash plate angle* α *(case 2).*

416

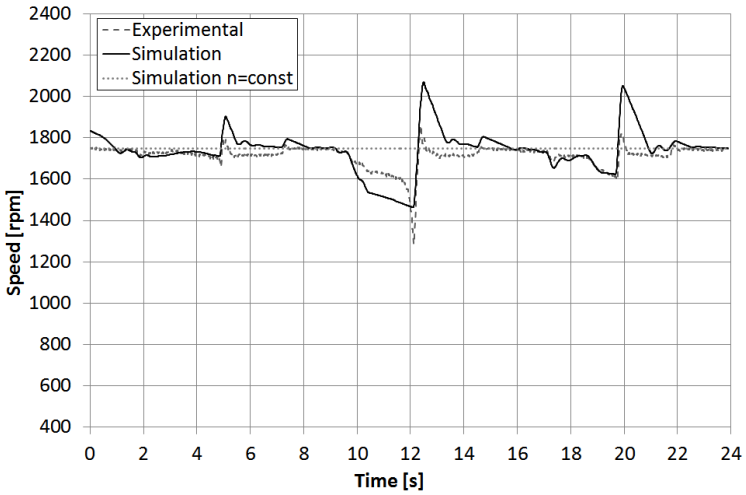

Fig.29. *Measured and calculated transients for engine speed (case 2).*

417

6. Conclusions

The paper is primarily aimed at the development of fast control-oriented simulation models of a typical mobile machinery, where hydraulic systems are coupled to internal combustion engines as prime movers. Hydraulic system model was built up within the AMESim® environment while the engine model was created in Simulink®. Results reported in the paper show how mathematical models of complex systems can be built up through co-simulation, i.e., merging proper sub-models even if from different modelling environment. Major difficulties that had to be solved in the presented work were related to the definition of integration time steps of merged sub-models, since they had to be chosen taking account of their numerical "stiffness" (significantly different when dealing with gaseous or liquid fluids). Notwithstanding the use of different time steps, the comprehensive model proved to run on a current PC faster than Real-Time. The comparison of calculated results with experimental data from a dedicated investigation showed that the model is able to predict system behaviour during fast transients with errors lower than 10% (with reference to pressures, engine speed and swash plate angle). The methodology adopted to formulate the model of the excavator can be used for control-oriented applications as a mathematical tool in the three typical levels of the optimization process, i.e.: definition of the optimal configuration of the system, since modularity of the model allows to change easily the layout of the system to investigate how it affects the overall behaviour; selection of the best size of all components, for the reason that all sub-models are physical-based and therefore can be easily modified; design of an optimized control strategy for the system through an easy link of the system model with the control unit(s) model(s), since the architecture of the overall model allows its implementation in MiL, SiL and HiL system widely used to define, test and optimize Electronic Control Units. The main advantage of the proposed co-simulation approach based on matching models from different environments is the use of the same tools to comply with each one of the mentioned level thus leading to a reduction of development time and costs and to a better understanding of the behaviour of the whole system. To this extent improvements considered for further development of the methodology will involve the application of the proposed modelling techniques to enhanced layouts (e.g., hybrid systems with hydraulic storage) and the implementation of the models in a real SiL/HiL system.

Acknowledgments

The authors would like to acknowledge the active support of this research by Casappa S.p.A., Parma and Walvoil S.P.A (ITALY).

References

[1] T.Costlow, "Making sense of hybrids", SAE Off-Highway Engineering, april 2014.
[2] M.Inderelst, S.Losse, S.Sigro, H.Murrenhoff, "Energy efficient system layout for work hydraulics of excavators.", 12th Scandinavian International Conference on Fluid Power, 2011, Tampere, Finland. ISBN 978-952-15-2520-9.
[3] G.Altare, D.Padovani, N.Nervegna, "A Commercial Excavator: Analysis, Modelling and Simulation of the Hydraulic Circuit.", SAE Technical Paper 2012-01-2040, 2012, doi:10.4271/2012-01-2040.
[4] M.Erkkilä, F.Bauer, D.Feld, "Universal Energy Storage and Recovery System – A Novel Approach for Hydraulic Hybrid", The 13th Scandinavian Int.Conf.on Fluid Power, SICFP2013, 2013, Linköping, Sweden.

[5] K.Renz, K.-H. Vogl, M.Brand, "Hydraulic Energy Storage for Hydrostatic Travel Drives", ATZ Magazine, Special edition on Energy Storage, pp.62-70.
[6] M.Conrad, "Hydraulic Hybrid Vehicle Technologies", Clean Technologies Forum, Sacramento, USA, 2008.
[7] S.Hui, Y.Lifu, J.Junqing, L.Yanling, "Control strategy of hydraulic/electric synergy system in heavy hybrid vehicles", Energy Conversion and Management, vol.52, 2011, pp. 668–674.
[8] D.Feng, D.Huang, D.Li, "Stochastic Model Predictive Energy Management for Series Hydraulic Hybrid Vehicle", Proceedings of the 2011 IEEE International Conference on Mechatronics and Automation, Beijing, China, 2011.
[9] T.H.Ho, K.K.Ahn, "Design and control of a closed-loop hydraulic energy-regenerative system", Automation in Construction, vol.22, 2012, pp.444–458.
[10] B.Wu, C.-C.Lin, Z.Filipi, H.Peng, D.Assanis, "Optimal Power Management for a Hydraulic Hybrid Delivery Truck", Vehicle System Dynamics, 2004, Vol.42, No.1–2.
[11] Z.Filipi, Y.J.Kim, "Hydraulic Hybrid Propulsion for Heavy Vehicles: Combining the Simulation and Engine-In-the-Loop Techniques to Maximize the Fuel Economy and Emission Benefits", Oil & Gas Science and Technology–Rev.IFP, Vol.65 (2010), No.1, pp.155-178, doi:10.2516/ogst/2009024.
[12] F.A.Bender, M.Kaszynski, O.Sawodny, "Location-Based Energy Management Optimization for Hybrid Hydraulic Vehicles", 2013 American Control Conference (ACC), Washington, USA, 2013.
[13] K.Patil, S.K.Molla, T.Schulze, "Hybrid Vehicle Model Development using ASM-AMESim-Simscape Co-Simulation for Real-Time HIL Applications", SAE paper no. 2012-01-0932, 2012, doi:10.4271/2012-01-0932.
[14] I.Cosadia, J.J.Silvestri, I.Papadimitriou, D.Maroteaux, P.Obernesser, "Traversing the V-Cycle with a Single Simulation - Application to the Renault 1.5 dCi Passenger Car Diesel Engine", SAE technical paper no.2013-01-1120.
[15] P.Casoli, A.Anthony, "Gray box modeling of an excavator's variable displacement hydraulic pump for fast simulation of excavation cycle", Control Engineering Practice, vol.21, pp.483-494, Elsevier, 2013, http://dx.doi.org/10.1016/j.conengprac.2012.11.011.
[16] A.Gambarotta, G.Lucchetti, I.Vaja, "Real-time Modelling of Transient Operation of Turbocharged Diesel Engines." 2011, Proc. I.Mech.E., Part D: Journal of Automobile Engineering, Vol. 225, ISSN 0954-4070.
[17] P.Casoli, A.Gambarotta, N.Pompini, U.Caiazzo, E.Lanfranco, A.Palmisano, "Development and validation of a "crank-angle" model of an automotive turbocharged Engine for HiL Applications", Energy Procedia, Elsevier, 2014, doi: 10.1016/j.egypro.2014.01.089.
[18] P.Casoli, A.Anthony, L.Riccò, "Modeling of an Excavator System – Load sensing flow sharing valve model", SAE 2012 Commercial Vehicle Engineering Congress, Rosemont, Illinois, USA, 2012, doi:10.4271/2012-01-2042.
[19] D.McCloy, H.M.Martin, "The control of Fluid Power", Hellis Horwood Limited, London, 1973, ISBN 0-85312-135-4.
[20] P.Casoli, A.Vacca, G.Franzoni, G.L.Berta, "Modeling of fluid properties in hydraulic positive displacement machines.", Elsevier, Simulation Modeling Practice and Theory, vol.14, Issue 8, November 2006, pp.1059-1072 ISSN: 1569-190X. doi:10.1016/j.simpat.2006.09.006.
[21] M.Zecchi, M.Ivantysynova, "Cylinder Block/Valve Plate Interface – a Novel Approach to Predict Thermal Surface", 8th International Fluid Power Conference, Dresden, March 26-28, 2012.
[22] M.Borghi, E.Specchia, B.Zardin, "Numerical Analysis of the Dynamic Behaviour of Axial Piston Pumps and Motors Slipper Bearings", SAE International Journal of passenger cars - Mechanical System, vol.2, pp.1285-1302, ISSN: 1946-3995, 2009.
[23] M.Pelosi and M.Ivantysynova, "A new Fluid-Structure Interaction Model for the Slipper-Swash Plate Interface.", Proc.5th FPNI Ph.D. Symposium, Cracow, Poland, pp.219-236, 2008.
[24] P. Casoli, A. Gambarotta, N. Pompini, L. Riccò (2014). "Development and application of co-simulation and control-oriented modeling in the improvement of performance and energy saving

of mobile machinery", Energy Procedia, Volume 45, 2014, Pages 849–858. Elsevier. http://dx.doi.org/10.1016/j.egypro.2014.01.090. Codice Scopus: 2-s2.0-84893640233.
[25] L.Guzzella, C.H.Onder – "Introduction to Modelling and Control of Internal Combustion Engine Systems." – Springer-Verlag, Berlin, 2010.
[26] L.Guzzella, A.Amstutz, "Control of Diesel engines", IEEE Trans.on Control Systems Tech., vol.18 (5), 1998.
[27] N.Watson, M.S.Janota – "Turbocharging the internal combustion engine" – John Wiley and Sons, 1982.
[28] J.B.Heywood – "Internal Combustion Engines Fundamentals" – McGraw-Hill, New York, 1988.
[29] O.E.Doebelin, "System Dynamics: modelling, analysis, simulation, design", Marcel Dekker Ed., New York, 1998.
[30] D.Anguita, P.Casoli, M.Canova, A.Gambarotta, F.Rivieccio – "A learning-machine based method for the simulation of combustion process in automotive I.C.Engines" – Spring Conference of the I.C.Engines Division of the ASME, paper no.ICES2003-682, Salzburg, 2003.
[31] J.Sun, I.Kolmanovsky, J.A.Cook, J.H.Buckland, "Modeling and Control of Automotive Powertrain Systems: a Tutorial", American Control Conference, Portland, June 2005.
[32] M.Canova, P.Fiorani, A.Gambarotta, M.Tonetti – "A real-time model of a small turbocharged Multijet Diesel engine: application and validation." – Proc.7th SAE-NA Int.Conf.on Engines for Automobiles, SAE paper no.2005-24-65, Capri, 2005.
[33] P.Fiorani, A.Gambarotta, E.Lanfranco, M.Tonetti – "A real-time model for the simulation of transient behaviour of automotive Diesel engines." – Proc.ATI/SAE Congress "The sustainable mobility challenge", SAE paper no.2006-01-3007, Perugia, 2006.
[34] A.Gambarotta, G.Lucchetti, M.Taburri, I.Vaja – "Mean Value Modeling of intake and exhaust systems of automotive engines: models identification and related errors" – 10th Stuttgart International Symposium on Automotive and Engine Technologies, Stuttgart, 2010.
[35] A.Gambarotta, G.Lucchetti, I.Vaja, "Real-time Modelling of Transient Operation of Turbocharged Diesel Engines", Proc. I.Mech.E., Part D: J. Automobile Engineering, Vol. 225, 2011, ISSN 0954-4070, DOI:10.1177/0954407011408943.
[36] Robert Bosch GmbH, "Diesel engine management", John Wiley & Sons, 2006.
[37] LMS Imagine, AMESim® Reference manual 2011.
[38] M.Tharayil and A.Alleyne. A generalized pid error governing scheme for SMART/SBLI control. IEEE American Control Conference, 1: 346-351, May 2002
[39] LMS Imagine.Lab AMESim. Activity Index REV13 User's Guide
[40] Louca L.S. "Modal analysis reduction of multi-body systems with generic damping", Journal of Computational Science 5 (2014) 415–426. doi:10.1016/j.jocs.2013.08.008].

Definitions

m	mass
n	rotational speed (in [r/min])
p	pressure
t	time
T	torque
V	volume
ρ	fluid density
η	efficiency

Subscripts

d	displacement
hm	hydro-mechanical
v	volumetric

Acronyms

F&E	Filling-and-Emptying
HHS	Hydraulic Hybrid System
ICE	Internal Combustion Engine
LS	Load-Sensing
MVM	Mean Value Model
QSF	Quasi Steady Flow

569 XiL Model-in-the-Loop (MiL), Software-in-the-Loop (SiL), Hardware-in-the-Loop (HiL),